Integration of SWAT and Remote Sensing Techniques to Simulate Soil Moisture in Data Scarce Micro-watersheds: A Case of Awramba Micro-watershed in the Upper Blue Nile Basin, Ethiopia

Berhanu G. Sinshaw[1(✉)], Mamaru A. Moges[2], Seifu A. Tilahun[2], Zoi Dokou[3], Semu Moges[3], Emmanouil Anagnostou[3], Daniel G. Eshete[1], Agumase T. Kindie[1], Engudye Bekele[2], Muludel Asese[2], and Wondale A. Getie[2]

[1] Department of Hydraulic and Water Resource Engineering, IOT, University of Gondar, P.O. Box 196, Gondar, Ethiopia
berhanugeremew0@gmail.com
[2] Faculty of Civil and Water Resource Engineering, BiT, Bahir Dar University, 26, Bahir Dar, Ethiopia
[3] Department of Civil and Environmental Engineering, University of Connecticut, 261, Glen-Brook Road, Storrs, CT 06269, USA

Abstract. Understanding soil moisture at a small scale is beneficial for predicting productivity and management of both rained and irrigated agriculture in mostly smallholder communities. This study aims to accurately represent micro-watershed scale soil moisture using the optimization capability of SWAT (SUFI2) model and soil information derived from Sentinel 2 A level 1 C satellite images with OPtical TRApezoid Model (OPTRAM) and MNDWI. The study was carried in the 700 ha Awramba watershed in the Upper Blue Nile, Ethiopia. Calibration and validation of SWAT were performed using in-situ stream flow data to enable the accurate simulation of water balance components such as soil moisture. The spectral water index was evaluated using MNDWI from the green band (560 nm) and short wave infrared band (2190 nm). The Results were evaluated based on the runoff response n and soil moisture fit to measured values. The runoff fit against the measured data using Nash Sutcliffe Efficiency (NSE) and R^2 criteria is 0.7 is and 0.75, respectively. The simulated daily soil moisture against the in-situ constant soil moisture provided NSE = 0.51, R^2 = 0.77, RMSE = 0.19 and PBIAS = −0.242. The simulation results indicate that validation of SWAT, OPTRA M and MNDWI models with in situ soil moisture data leads to acceptable accuracy with 0.0027 cm^3 cm^{-3}, 0.0022 cm^3 cm^{-3} and 0.034 cm^3 cm^{-3} standard errors, respectively. Furthermore, Sentinel 2A imagery is found to have a higher potential to simulate soil moisture compared to TDR data. The overall study indicates satellite-based soil moisture provides an encouraging pathway to setting up soil moisture-based prediction for smallholder agriculture in Ethiopia.

Keywords: Sentinel -2 · OPTRAM · SWAT · TDR · Gravimetric method · Soil moisture

N. G. Habtu et al. (Eds.): ICAST 2019, LNICST 308, pp. 294–314, 2020.
https://doi.org/10.1007/978-3-030-43690-2_20

1 Introduction

1.1 Background

Globally, 65% of water received as precipitation returns to the atmosphere as green water flow and the rest remain in the soil and flow as a runoff. The green water storage (soil moisture) is the amount of water in the soil profile at the end of a period [1]. Surface soil moisture controls the partition of rainfall into runoff, infiltration and other hydrological variables. Soil moisture directly influences the rate of evaporation, groundwater recharge and runoff generation and has an essential influence on climate [2]. Soil moisture can be estimated using in situ networks, hydrological models and remote sensing technique. However, an integrated approach can overcome the drawbacks of every single method and produce more big data [3]. Traditional in situ measurements provide valuable information at different soil depths. Many field techniques are available including; gravimetric, tension measuring, neutron probe, Time Domain Reflectometry (TDR) and capacitance measurements [4]. Hydrological SWAT model can estimate soil moisture in HRU/sub-basin/level up to vertical root depth (60 cm) of plants. For the data-scarce region, the model effectively calibrated and validated using stream flow data for the proper partition of hydrological water balance components [5].

Remote sensing technique enables to monitor soil moisture over a large area. The recently launched Sentinel two satellite has the potential to improve soil moisture product up to a resolution of 10 m. Soil moisture content is a critical hydrological and climatic variable in various application domains but the retrieval from local direct measurements of distributed, quantitative and accurate information relative to the moisture level of soils on a global scale is almost impracticable, due to the high spatial variability of the target variable, time, and expensive nature of devices. Sustainable agriculture and water resource management need accurate information on surface soil moisture. Low soil moisture for sustained periods results in drought and plant water deficit and potentially leading to wild Fire [6].

Conversely, high soil moisture leads to increased risk of flood. Also, the evaporation rate is strongly correlated to soil moisture that makes a secure connection between the land surface and atmosphere [7]. Continuous observation of soil moisture is difficult in a large area, but we can monitor effectively and conveniently by using remote sensing technology. Despite the importance of soil moisture, in situ measurement is very difficult and requires resources, both labour and finance. The only limited area can be controlled by in situ point observation, which cannot be representative for the broader region. Nowadays, direct views of soil moisture were restricted to discrete measurements at a specific location, and such point-based measures do not represent the spatial distribution, because soil moisture is highly variable both in spatially and temporal scale. The depth at which soil moisture is sensed by satellites depends on the sensor frequency but usually does not exceed 30 cm in order to access root zone soil moisture hydrological model is needed and several approaches have been developed such as techniques based on the energy balance approach based on thermal infrared soil moisture or simplified water balanced approaches [8]. Passive remote sensing instruments can be used to determine

the surface soil moisture with a temporal resolution of different days. The European Space Agency (ESA) Soil Moisture and Ocean Salinity (SMOS) mission [9] and the National Aeronautics and Space Administration (NASA) Soil Moisture Active and Passive (SMAP) mission have a low spatial resolution around 25 km. According to [10] the current Sentinel-2 purpose, active onboard C-band sensor offers regular temporal coverage (about five days for both A and B satellites) together with a spatial resolution of 10 m from the optical image.

1.2 Objective

1.2.1 General Objective

- The main aim of the study is to simulate soil moisture using SWAT and Remote Sensing Techniques in Data Scarce Micro-Watersheds.

1.2.2 Specific Objective

- To simulate spatial and temporal soil moisture content using SWAT hydrological model at sub-basin level
- To generate a time series satellite image-based soil moisture index from Sentinel 2 A images
- To evaluate satellite-based water index from Sentinel 2 A picture with in situ soil moisture data.

2 Materials and Methods

2.1 Description of the Study Area

The study was carried out in upper Blue Nile, Ethiopia, in small watershed called Awramba. Geographically located between 11.886^{o} N–11.9253^{o} N and 37.781^{o} E–37.806^{o} E having elevation difference between 1887 m and 2305 m above sea level. It located in the south-east of part Lake Tana, 75 km North West of Bahir Dar city. Awramba watershed covers an area of 700 ha that receive 1497 mm rainfall depth and **21 ^{o}C** average temperature (Fig. 1).

Soil type: In Awramba, the type of soil is volcanic in origin range from mainly clay texture throughout the mid and down slope positions (near the outlet) and clay to sandy clay soils on the top slopes [22]. More than 99% of the watershed based on the classification of the Food and Agriculture Organization (FAO) consists of Haplic Luvisols.

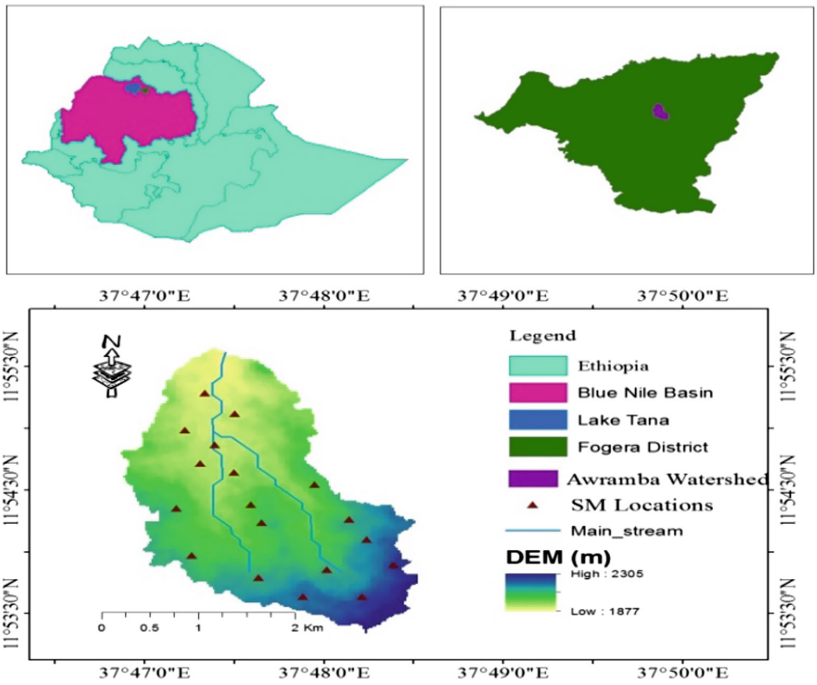

Fig. 1. Location map of Awramba watershed

2.2 Materials

The materials used for this study were presented in (Tables 1 and 2).

Table 1. Different data sources used for this study

No	Type data	Source	Purpose
1	STRM DEM	https://earthexplorer.usgs.gov/	Delineation and slope map
2	Soil	MoWRIE	Soil map
3	Sentinel 2 image	(https://scihub.copernicus.eu/dhus/# /home)	OPTRAM, MNDWI and LULC map
4	Weather data	Metrological stations	Input for the SWAT model

Soil Moisture: In-situ soil moisture measurements were collected seven-day basis over 2017/2018 at 18 representative locations in the Awramba watershed. In-situ soil moisture observations collected for SWAT model and satellite soil moisture product validation purpose. In each site, the measurement was carried out at 10 cm depth using TDR. The assembled TDR probe soil moisture products calibrated with commonly used gravimetric soil moisture content.

Table 2. Different decision support tools used for this study and their purposes

No	Software name	Purpose
1	Arc GIS 10.1	Preparation of daily soil moisture maps
2	ENVI 5.1	Lee sigma filtering and image enhancement
3	EndNote X6	Citation and references
4	SNAP 6.0	Sentinel 2 image-processing, NDVI and MNDWI
5	Arc SWAT 2012	Act as a GIS interface for SWAT modeling
6	WAGEN.excel macro	Weather generator preparation
7	dew02.exe	Monthly dew point computation
8	XLSTAT	Hydrological data quality
9	SWAT CUP 2012	SWAT calibration, validation and sensitivity analysis

2.3 Soil Moisture Estimation Models

2.3.1 Soil and Water Assessment Tool (SWAT)

It is a physical based semi-distributed basin scale model that uses different data such as DEM, soil, land use, and climatic data for hydrological and climatological modeling on the daily or monthly bases [11]. The model includes weather, hydrology, soil properties, and plant growth, nutrients, and land management practices. The first stage of-of modeling involves watershed delineation. The delineated watershed further subdivided into hydrologic response units (HRU), which is a unique combination of land use management, soil, and slope. Each HRU in the model behaves differently for precipitation and temperature input [12].

The conversion of sub-basin to the single basin made by changing the threshold limit in the model. After simulating SWAT output, soil moisture (m^3 m^{-3}) determined by using Eq. 1.1

$$\Delta \mathrm{SMC} = \sum_{i=1}^{t} (\mathrm{Rday} - \mathrm{Qsurf} - \mathrm{Ea} - \mathrm{Wseep} - \mathrm{Qgw}) \tag{1.1}$$

Where; SW_T is the final soil water content (mm), Rday is the simulation time (days), R_{ay} is the amount of daily precipitation (mm), Qsurf is the amount of daily surface runoff (mm), Ea is the amount of daily evapotranspiration (mm), Wseep is the amount of water entering into the vadose zone from the soil profile on a given day (mm), and Qgw is the amount of return flow on a given day (mm).

2.3.2 SWAT Model Calibration and Validation

An automatic SWAT- CUP computer program was implemented for calibration and validation of the SWAT model. This program links GLUE, Parasol, SUFI 2, and MCMC and PSO procedures to SWAT. It enables sensitivity analysis, calibration and validation of SWAT model parameters. This method uses a Bayesian framework to determine the uncertainties with a sequential uncertainty fitting process in which iteration and unknown

parameter estimates were achieved before final forecast. It considers difficulties of model input, structure, parameters and observed data. Global Sensitivity analysis method (using t-Stat and p-Value to assess sensitivity) during the calibration process was to avoid the equifinality phenomenon.

2.4 Sentinel Image Soil Moisture Estimation

Sentinel-2 is a European wide-swath, high-resolution, multi-spectral imaging mission. The full mission specification of the twin satellites flying in the same orbit but phased at 180°, is designed to give a high revisit frequency of 5 days at the equator. Sentinel-2 carries an optical instrument payload that has 13 spectral bands: four bands at 10 m, six bands at 20 m and three bands at 60 m spatial resolution. The novel optical trapezoid model is a physical based model designed to estimate soil moisture content from a visual image by replacing Land surface temperature from a thermal band with a measure for soil moisture in the optical domain develop OPTRM from flux radiative transfer model formulate a physical model that exhibits a linear relationship between surface soil moisture content and SWIR transformed reflectance using Eq. 1.2 [13, 14]

$$\mathrm{SMI} = \frac{\theta - \theta\mathrm{d}}{\theta\mathrm{w} - \theta\mathrm{d}} = \frac{\mathrm{STR} - \mathrm{STRd}}{\mathrm{STRw} + \mathrm{STRd}} \tag{1.2}$$

Where STR is the SWIR transformed reflectance, $\mathrm{STR_d}$ and $\mathrm{STR_w}$ are STR at θd and θw respectively. The STR is related to SWIR reflectance, RSWIR, computed using Eq. 1.3

$$\mathrm{STR} = \frac{(1 - \mathrm{RSWIR})^2}{2\mathrm{RSWIR}} \tag{1.3}$$

Based on the assumption of a linear relationship between soil and vegetation water contents, we expect that the STR-NDVI space forms a trapezoid as well. Therefore, the parameters of the can are obtained for a specific location from the dry and wet edges of the optical trapezoid using linear regression system determined using Eqs. 1.4 and 1.5

$$\mathrm{STR_d} = \mathrm{i_d} + \mathrm{S_d NDVI} \tag{1.4}$$

$$\mathrm{STR_w} = \mathrm{i_w} + \mathrm{s_d NDVI} \tag{1.5}$$

The normalized difference water index (NDVI) computed from band 4 (Red) and band 8 (NIR) using Eq. 1.6;

$$\mathrm{NDVI} = \frac{\mathrm{NIR} - \mathrm{Red}}{\mathrm{NIR} + \mathrm{Red}} \tag{1.6}$$

Where; NIR is the TOA reflectance value of the NIR band (band 8), and red is the TOA reflectance value of the red group (group 4). The freely available sentinel -2 Levels 1C dataset is a standard product of TOA reflectance [15].

The NDVI was determined from the contribution of visible and NIR band. Healthy and well-nourished vegetation absorbs most of the visible wavelengths and reflects a large proportion of NIR light, whereas sparse plant reflects more visible wavelength

light and less NIR light. Combining Eqs. 1.4 and 1.5, the soil moisture for each pixel can be estimated as a function of STR and NDVI determined as Eq. 1.7

$$\mathrm{SMI} = \frac{\mathrm{id} + \mathrm{SdNDVI} - \mathrm{STR}}{(\mathrm{id} - \mathrm{iw}) + (\mathrm{sd} - \mathrm{sw})\mathrm{NDVI}} \tag{1.7}$$

Where; i_d and s_d are dry parameters of NDVI – STR scatter plot, i_n and SW are wet parameters of NDVI – STR scatter plot and NDVI is the average vegetation index of the satellite. The Sentinel 2A level 1 C band 12 images with 20 m spatial resolutions were resample to 10 m resolution with the nearest neighbor method to match the spatial resolutions of group 4 and 8.

2.4.1 OPTRA M Model Validation and Sensitivity Analysis

The parameter removal sensitivity analyses, according to [16, 17] and [18] were used to identify the factors that profoundly affect the soil moisture content.

$$\mathrm{s} = \left[\frac{\frac{\mathrm{SM}}{\mathrm{N}} - \frac{\mathrm{SM}'}{\mathrm{n}}}{\mathrm{SM}} \right] \tag{1.8}$$

where; S is Sensitivity index analysis associated with the removal of one parameter; SM is the soil moisture index computed using all the settings; SM′ is the soil moisture index calculated by excluding one thematic parameter at a time; N a n are the numbers of parameters used to calculate SM and SM′ respectively.

2.4.2 Satellite Data Bias Correction

The bias from satellite image soil moisture retrieval was removed using cumulative density function CDF function.

$$\theta = \mu_{\mathrm{ground}} + \frac{\sigma\,\mathrm{sat} + \sigma\,\mathrm{ground}}{2} \times \frac{Sat - \mu\mathrm{sat}}{\sigma\,\mathrm{sat}} \tag{1.9}$$

Where; θ is the final corrected soil moisture, the μ_{ground} ground is in situ soil moisture, σ_{sat} is the standard deviation of satellite soil moisture, the σ_{ground} is the standard deviation of in situ soil moisture, sat is satellite soil moisture, sat is satellite soil moisture.

2.4.3 Spectral Water Index Extraction Using MNDWI

The spectral Normalized difference water index proposed by [19] designed to maximize the reflectance of the water body in the green band and minimize the reflectance of the water body in the NIR band. McFeeters's NDWI determined as;

$$\mathrm{NDWI} = \frac{\rho\mathrm{Green} - \rho\mathrm{NIR}}{\rho\mathrm{Green} + \rho\mathrm{NIR}} \tag{2.0}$$

Where; ρGreen is the TOA reflectance value of the green band and ρNIR is the TOA reflectance value of the NIR band. Comparing to the raw Digital Numbers (DN), TOA reflectance is more suitable in calculating NDWI. The freely available Sentinel 2A Level 1C dataset is already a standard product of TOA reflectance. Therefore, no additional pre-processing is required.

2.4.4 Model Performance Evaluation

Based on [19], four quantitative statistics were used to assess model performance in catchment simulation (Table 3).

Table 3. SWAT model performance range

Rank	NSE	PBIAS	RMSE
Very good	$1 \geq \text{NSE} \geq 0.75$	$\text{PBIS} < 10$	$0 \leq \text{RMSE} \leq 0.5$
Good	$0.75 \geq \text{NSE} \geq 0.65$	$15 \geq \text{PBIS} > 10$	$0.5 \leq \text{RMSE} \leq 0.6$
Satisfactory	$0.65 \geq \text{NSE} \geq 0.5$	$25 \geq \text{PBIS} > 15$	$0.6 \leq \text{RMSE} \leq 0.7$

3 Results and Discussion

3.1 Land Use Land Covers Classification

Thirty-four ground truth spatial points were used to classify pixel based land use land cover classification.

According to Table 4, the image classified in to four major classes; agriculture (3.53 km^2), forest (2.21 km^2), grassland and shrubs (1.16 km^2) and village (0.067 km^2). Agriculture was the dominant type of land use practice which covers half of the total area of the watershed. The study had an overall classification accuracy of 85.5% and a kappa coefficient of 80% that indicated very good classification (Fig. 2).

Table 4. Performance evaluation of Sentinel 2 for land LULC classification

Land use	Producer accuracy (%)	Omission error (%)	User accuracy (%)	Commission error (%)	Overall accuracy (%)	Kappa coefficient (%)
Cultivated	82	18	90	10	85	80
Village area	100	0	83	17		
Forest land	71	29	71	29		
Grass land	91	9	91	9		

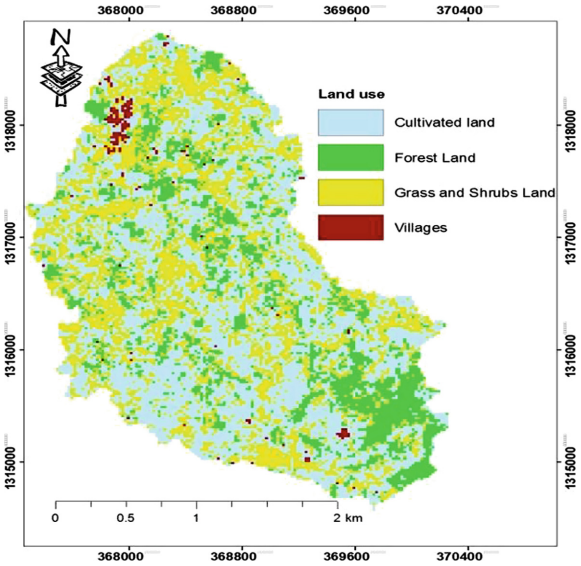

Fig. 2. Land use of Awramba classified from sentinel two images

3.2 SWAT Model Configuration

The SWAT model has configured with DEM 30 m resolution and discredited based on the maximum areal threshold value into 330 Hydrological Response Unit (HRU) and 35 sub-basins to get detail information about the topographic characteristics. The maximum area of the sub basin was 1.732 Km^2 (sub basin 32), and the minimum was 0.0164 Km^2 (sub basin 8). The HRUs were defined using land use, soil and slope with a threshold value of 10%, 20%, 10% respectively [20]. The input tables were defined based on the daily time step climatic data collected from within and around the watershed with their relevant location files. The model was run from 2013–2017 seasons by considering 2013 data to warm up the model and the rest three and one year's data were considered as calibration and validation at the outlet point using stream discharge daily observation.

During the simulation of the SWAT model, there was a discrepancy between measured data and simulated results. Therefore, to minimize this inconsistency, selecting sensitive parameters which affect the outcome and the extent of variation is mandatory for better hydrological modeling. Global sensitivity analysis in SWAT CUP 2012 is the favorite tool to show the rank and relative sensitivity. In the present study, initially, 30 parameters were used to know the status of each parameter. Among the 30 benchmarks, the top nineteen parameters were used for the calibration and validation process. Parameter sensitivity and ranking in SWAT CUP was measured using the t-stat and p-values. Where t-stat is the coefficient of a parameter divided by its standard error. The p-value is used to determine the significance of the sensitivity. Parameters are significant for a larger absolute t-stat and lower p-values. The T-stat measures sensitivity with larger absolute values, while the P-value considers zero cost to determine sensitivity [21]. A more significant p-value suggests that changes in the predictor values are not associated with changes in the response variable.

3.3 Sensitivity Analysis, Calibration and Validation of SWAT Model

According to Global sensitivity analysis result indicates that curve number II, alpha base flow recession constant, and groundwater delay were the three top sensitive parameters that determine the water balance of Awramba catchment. The sensitivity rank is in line with [20, 22] tested in the upper Blue Nile basin. Curve number method is one of the most popular ways for computing the runoff volume from a rainstorm. Soil and groundwater parameters are found to be the most sensitive parameters in lowland catchments [23] (Table 5).

Table 5. SWAT parameters used for calibration and their sensitivity ranks in Awramba

Parameter Name	File Extra	Fitted Value	Min Value	Max Value	t Stat	P Value	Sensitivity Rank
R__CN2	mgt	−0.165	−0.2	0.2	−29.2	0	1
V__ALPHA_BF	Gw	0.104	0	1	−0.28	0.78	2
V__GW_DELAY	Gw	164.583	0	500	1.51	0.14	3
V__GWQMN	Gw	1437.5	0	5000	−0.16	0.88	4
R__ESCO	hru	0.188	0	1	1.55	0.12	5
R__ESCO	bsn	0.671	0	1	−0.64	0.52	6
R__CH_N2	rte	0.021	0	0.3	−0.03	0.98	7
R__CH_K2	rte	95.104	5	130	−1.77	0.08	8
R__SOL_AWC	sol	0.283	−0.2	0.4	0.13	0.9	9
R__SOL_BD	sol	0.138	−0.5	0.5	2.54	0.01	10

3.4 SWAT Stream Flow Modeling

Stream discharge in Awramba watershed was collected from 2013–2017 for watershed management evaluation purpose in daily time step. The rating curve developed by [22] from 2013–2015 was used to estimate the discharge in 2016 and 2017. To evaluate the SWAT model performance stream-discharge relationship at gage station historical time series data from 2013–2017 is considered. Calibration and validation were performed on measured stream flow from a gagging station for the year 2014–2016 and 2017 respectively (Tables 6, 7 and Fig. 3).

Table 6. Daily stream flow modeling statistical performance

Flow (m^3/s)	p-factor	r-factor	R^2	NSE	PBIAS	RMSE
Calibration	1	0.64	0.75	0.7	−2.1	0.55
Validation	0.98	0.49	0.91	0.9	−9.7	0.31

Table 7. Monthly stream flow model performance

Flow (m^3/s)	R^2	NSE	PPBIAS	RMSE
Calibration	0.98	0.94	−16.432	1.07
Validation	0.97	0.96	−0.07367	1.075

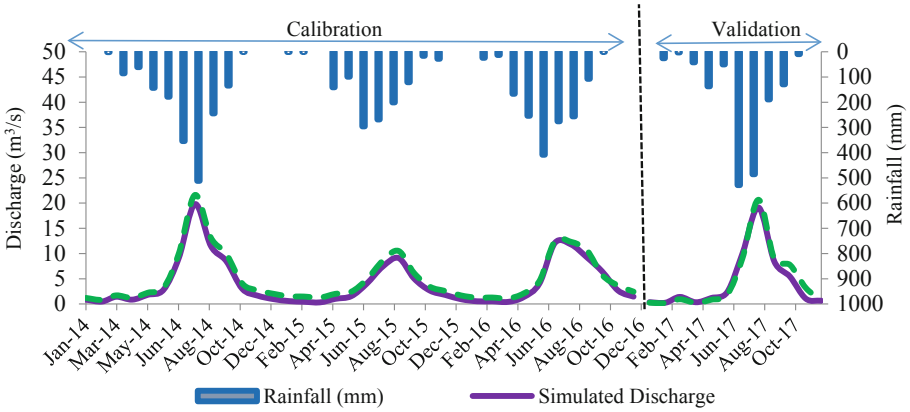

Fig. 3. Monthly stream flow (m^3/s) during calibration and validation versus monthly rainfall depth (mm)

3.5 SWAT Soil Moisture Modeling

The moisture content was calibrated and validated by stream flow data due to lack of long term gagged soil moisture data at sub-basin level because the simulation of soil moisture content using SWAT model is highly dependent on simulation of runoff generation process [24].

As indicated in (Fig. 4) SWAT model results the amount of soil moisture reduces from 2014–2017 with annual rainfall depth (Table 8).

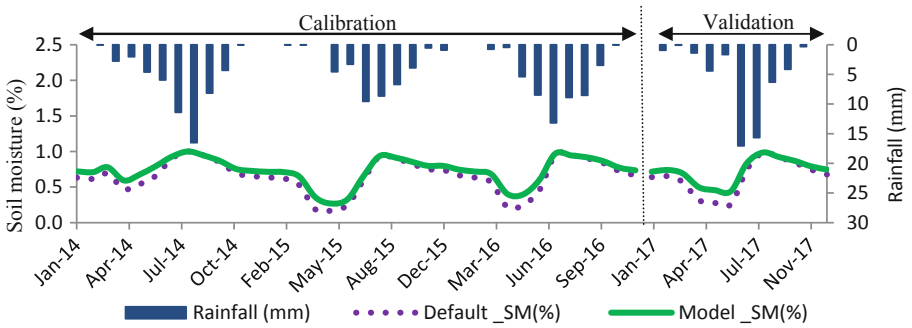

Fig. 4. SWAT monthly soil moisture during calibration and validation by using Stream flow data from 2014–2017

Table 8. Water balance of Awramba watershed using SWAT model (2014–2017)

Year	Rainfall	PET	ET	Q_GW	WYLD	SM	Q
	(mm)	(mm)	(mm)	(mm)	(mm)	(mm)	m^3/s
2014	1713.92	1233.6	560.3	355.96	1124.49	119.34	795
2015	1171.05	1339	569.6	193.4	575.22	98.34	447
2016	1505.53	1287.7	537.9	295.66	946.73	107.72	662
2017	1599.3	1306.7	597.4	281.52	972.35	105.15	649
Mean	1497.45	1291.7	566.3	281.64	904.7	107.64	638

The rainfall depth in 2014 was 1713 mm respond an average soil moisture value of 119.33 mm. In 2015 season, the rainfall depth was 1171.05 mm response 98.34 mm amount of water stored in root depth of the plant. The amount of rainfall in 2016 and 2017 were 1505 mm and 1599 mm, which responses 107.72 mm and 105.14 mm soil moisture content. SWAT modeling results indicated the amount of soil content around the watershed was determined by the amount of rainfall value directly. Both hydrological variables reduced with time, especially in 2015 there was a small amount of rainfall annually; as a result, the amount of water stored and available for plants were lower than the rest years. But, the partition of soil moisture from the total rainfall was higher in 2015 because the soil can absorb the incident rainfall by reducing runoff generation potential. SWAT model calibration using stream flow data improve the soil moisture product in daily time step.

3.6 Sentinel 2 Satellite Soil Moisture Estimation Methods

A physically-based trapezoidal space termed the "Optical TRApezoid Model" (OPTRAM) to estimate surface soil moisture remote from Sentinel two satellites based on optical data only [13]. The concept is based on the pixel distribution between STR-NDVI

spaces, where STR is the SWIR transformed reflectance, and NDVI is the Normalized difference vegetation index, thereby replacing LST in the conventional trapezoid model. Considering a linear relationship between soil moisture content, SMI (0 for completely dry and 1 for saturated soil) and STR [25] Normalized Difference Vegetation Index (NDVI): Most vegetation indices combine information contained from the red and near-infrared (NIR) spectral bands [26]. The index was higher in the rainy season and lowered in the dry season (April and May) (Fig. 5).

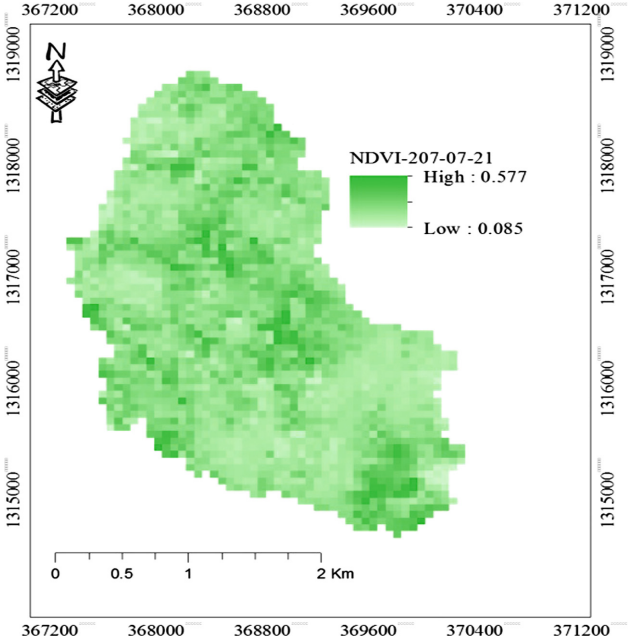

Fig. 5. Normalized difference vegetation index map

3.6.1 Shortwave Infrared Transformed Reflectance (STR) Map

Shortwave infrared transformed reflectance (STR) is one of the parameter used to determine the soil moisture status of a soil by replacing the land surface temperature (NDVI, LST) in thermal triangular model with a linear relationship between (NDVI, STR) in optical tripartite model because LST is computed from thermal band of the satellite imagery (Fig. 6).

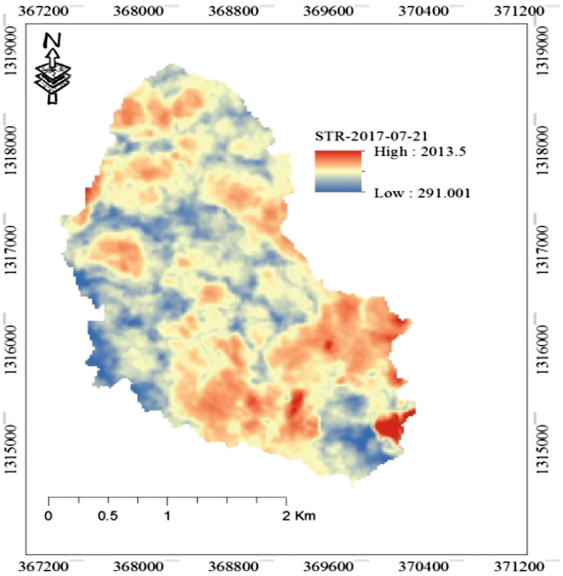

Fig. 6. STR maps from SWIR band

STR map in the study area varies both spatially and temporally in 2017 season. Most of the STR map result reveals that the highest elevation part of the watershed has a lower value of STR whereas lower elevation part of the basin was the higher value of STR like that of land surface temperature (Table 9 and Fig. 7).

Table 9. Daily OPTRA M parameters

Date	NDVI max	NDVI min	STR max	STR min	i_d	i_w	s_d	s_w
2-Jan-17	0.75	0.05	1326	239.5	190.5	1142.98	76.23	457.37
11-Feb-17	0.59	0.01	1450.5	287	262.88	1328.6	79.63	402.44
23-Mar-17	0.4	0.06	1242	455.5	433.27	1181.4	98.13	267.58
22-Apr-17	0.64	0	1528	350	317.18	1384.71	102.03	445.44
11-Jun-17	0.66	−0.08	3226	211.5	194.82	2971.51	57.01	869.62
1-Jul-17	0.58	0.12	1616.5	306	272.46	1439.3	95.6	505.02
21-Jul-17	0.58	0.09	2013.5	290	287.89	1510.18	24.63	871.84
30-Aug-17	0.55	0.13	2013.5	291	261.46	1809.06	87.89	608.14
29-Sep-17	0.79	0.15	1487.5	111.5	108.89	923.47	16.86	721.71
9-Sep-17	0.77	0.12	1280	154	128.62	1069.02	57.14	474.91
9-Oct-17	0.78	0.13	1823	221	182.88	1508.52	83.5	688.77
29-Oct-17	0.82	0	1266	203	173.66	1083.03	71.38	445.15
28-Nov-17	0.63	0.16	1719	212.5	183.71	1486.1	32.69	588.31
28-Dec-17	0.67	0.05	1591.5	233	206.28	1408.97	74.24	507.13

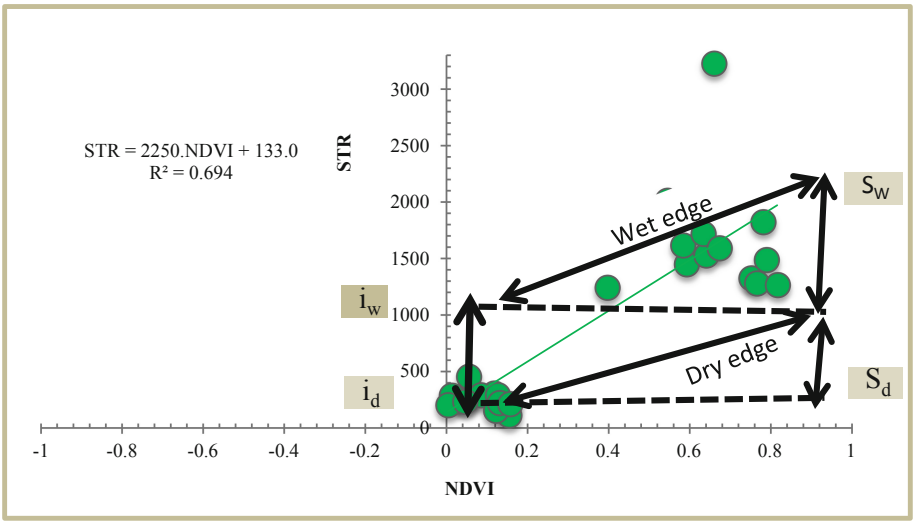

Fig. 7. Standardized rating curve between NDVI and STR

3.6.2 Sensitivity Analysis of Optical Trapezoidal Model Parameters

The highest variation index with mean −7.97 associated with soil moisture index value. Soil moisture index also sensitive to STR and NDVI with a mean variation index value of −1.09 and −1.01 respectively next to i_w. It is less susceptible to S_d and S_w with a mean variation of 0.19 and 0.02, respectively (Table 10).

Table 10. Map removal sensitivity analysis statistical value of the OPtical TRApezoidal Model

Date	NDVI	STR	i_d	i_w	s_d	s_w
2-Jan-17	−1.02	−1.08	−0.77	−30.1	0.03	0.2
11-Feb-17	−0.94	−1.1	−0.76	−8.05	0.02	0.12
23-Mar-17	−0.91	−1.23	−0.73	−2.99	0.03	0.08
22-Apr-17	−0.96	−1.12	−0.76	−6.7	0.03	0.14
1-Jul-17	−0.98	−1.09	−0.77	−11.2	0.02	0.16
29-Sep-17	−1.23	−1.03	−0.79	4.12	0	0.42
9-Oct-17	−1.07	−1.06	−0.78	16.14	0.02	0.24
29-Oct-17	−1.03	−1.08	−0.77	−54.1	0.03	0.21
28-Nov-18	−0.99	−1.05	−0.78	41	0.01	0.18
28-Dec-17	−0.97	−1.07	−0.77	−27.9	0.02	0.16
Average	−1.01	−1.09	−0.77	−7.97	0.02	0.19
Sensitivity rank	3	2	4	1	6	5

3.6.3 Soil Moisture Index Map

Mapping soil moisture index in small watershed level is difficult due to satellites poor resolution and quality of imagery. The Sentinel 2 A levels 1 C image has 13 spectral bands that can detect our environment in the different spectral band from 443 nm–2190 nm. Group 4 (665 nm) and band 8 (740 nm) were used for normalized difference vegetation index (NDVI) computation in sentinel application platform(SNAP Version 6.0), and the short wave infrared (SWIR) band 12 (2190 nm) was used for computing STR in band math. Finally, the soil moisture mapping process were done using OPtical TRApezoidal Model after calculating the daily dry edge (i_d and S_d) and wet edge (i_w and S_w) parameters in linear regression program using Microsoft excel solver. The daily time series dry and wet edge parameters are presented in Table 11 below (Fig. 8).

Table 11. Spatial and temporal MNDWI product in Awramba watershed

Date	2-Jan-17	11-Jan-17	23-Mar-17	22-Apr-17	12-May-17	11-Jun-17	1-Jul-17	30-Aug-17	9-Sep-17	9-Oct-17	28-Nov-17	8-Dec-17	Mean
SM_1	−0.44	−0.31	−0.32	−0.43	−0.28	0.02	−0.29	−0.09	−0.25	−0.28	−0.41	−0.44	−0.28
SM_2	−0.38	−0.38	−0.25	−0.34	−0.21	−0.1	−0.14	−0.01	−0.24	−0.28	−0.31	−0.34	−0.24
SM_3	−0.25	−0.22	−0.2	−0.23	−0.22	−0.07	−0.13	−0.02	−0.18	−0.25	−0.35	−0.34	−0.19
SM_4	−0.39	−0.26	−0.27	−0.39	−0.18	−0.23	−0.22	0	−0.2	−0.19	−0.43	−0.43	−0.25
SM_5	−0.29	−0.18	−0.24	−0.3	−0.2	−0.12	−0.15	−0.01	−0.24	−0.31	−0.39	−0.32	−0.22
SM_6	−0.26	−0.13	−0.18	−0.22	−0.18	−0.12	−0.03	−0.01	−0.18	−0.25	−0.3	−0.28	−0.17
SM_7	−0.3	−0.25	−0.18	−0.3	−0.18	−0.18	−0.17	−0.03	−0.11	−0.2	−0.33	−0.32	−0.2
SM_8	−0.34	−0.21	−0.23	−0.3	−0.16	−0.15	−0.04	−0.02	−0.16	−0.23	−0.28	−0.25	−0.19
SM_9	−0.35	−0.31	−0.25	−0.35	−0.17	−0.22	−0.17	−0.04	−0.24	−0.31	−0.35	−0.33	−0.25
SM_10	−0.25	−0.12	−0.18	−0.25	−0.17	−0.2	−0.13	−0.09	−0.15	−0.18	−0.25	−0.24	−0.18
SM_11	−0.22	−0.21	−0.18	−0.25	−0.16	−0.12	−0.11	−0.03	−0.15	−0.21	−0.3	−0.28	−0.18
SM_12	−0.21	−0.14	−0.15	−0.2	−0.18	−0.18	−0.14	0.05	0.04	−0.23	−0.3	−0.28	−0.15
SM_13	−0.29	−0.23	−0.2	−0.28	−0.16	−0.1	−0.13	0.06	−0.19	−0.23	−0.34	−0.32	−0.19
SM_14	−0.38	−0.15	−0.26	−0.36	−0.17	−0.25	−0.14	0.02	−0.19	−0.29	−0.4	−0.4	−0.23
SM_15	−0.21	−0.18	−0.14	−0.21	−0.2	−0.13	−0.09	−0.01	−0.15	−0.2	−0.23	−0.22	−0.16
SM_16	−0.28	−0.19	−0.19	−0.29	−0.16	−0.1	−0.16	−0.01	−0.21	−0.25	−0.27	−0.25	−0.19
SM_17	−0.31	−0.25	−0.2	−0.28	−0.18	−0.26	−0.14	−0.03	−0.11	−0.11	−0.18	−0.13	−0.19
SM_18	−0.25	−0.21	−0.19	−0.28	−0.29	−0.23	−0.14	0.04	−0.17	−0.22	−0.24	−0.21	−0.2
Mean	−0.3	−0.22	−0.21	−0.29	−0.19	−0.15	−0.14	−0.01	−0.17	−0.23	−0.31	−0.3	−0.2

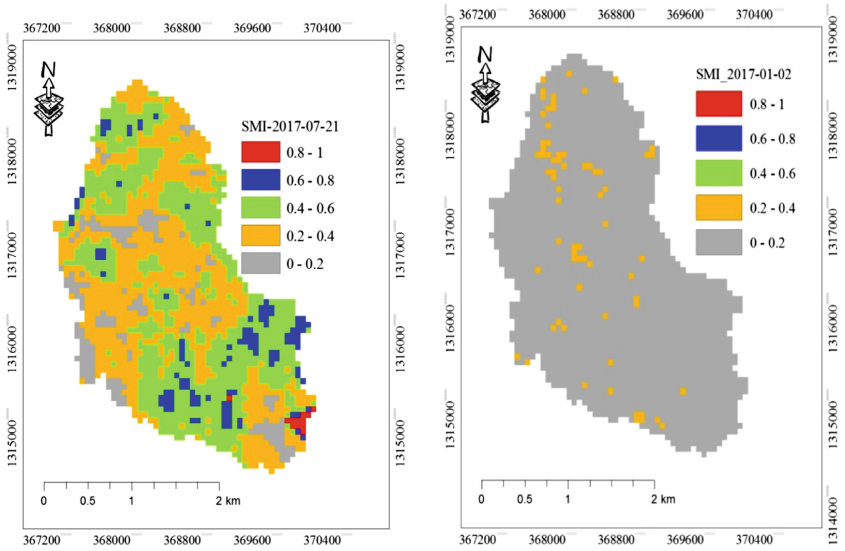

Fig. 8. Daily soil moisture maps estimated using OPTRAM

3.6.4 Bias Correction

There is a discrepancy in estimating soil moisture form sentinel 2 A satellite image. To account any bias between the two sets of data is removed using a simple cumulative density function (CDF) that the standard deviation of both the ground station data and the satellite data. The percentage bias was estimated at −0.094, which is very insignificant.

3.6.5 Spectral Water Index Extraction Using MNDWI

The average product of spectral water index is less than $-0.013\ cm^3\ cm^{-3}$ thus indicates that water is not the dominant land use coverage. Spectral water index approaches to zero in the rainy season especially July – end of September and lowers in the dry season in November – May. The average value of MNDWI (−0.212) was more significant than the average NDVI (0.3). The result is agreed with a five years analysis of MODIS image in the vast central plain of the United States (NDVI = 0.5 and NDWI = 0.3) [27]. The time series MNDWI data in (Fig. 9) indicates that water index was higher in the rainy season (June – September) and decline starting the dry season from October – May. The water index has a similar pattern with soil moisture time series data extracted from Sentinel 2 A image, but the product of soil moisture is higher than 0 $cm^3\ cm^{-3}$, and MNDWI is less than 0.

3.7 Model Accuracy Assessment

A comparison between SWAT, OPTRA M soil moisture and MNDWI spectral water index with in situ soil moisture measured at 10 cm depth data is depicted in Fig. 9. The result indicates that validation of three models with in situ soil moisture data generally leads to acceptable accuracy having 0.0027 $cm^3\ cm^{-3}$ and 0.0022 $cm^3\ cm^{-3}$

and 0.034 cm^3 cm^{-3} standard errors respectively. Overall, the accuracy of sentinel two images using OPtical TRApizoidal Model and SWAT hydrological model are grater then MNDWI spectral water index. All models were agreed with result of soil moisture content less than 0.04 cm^3 cm^{-3} standard error [13] (Table 12).

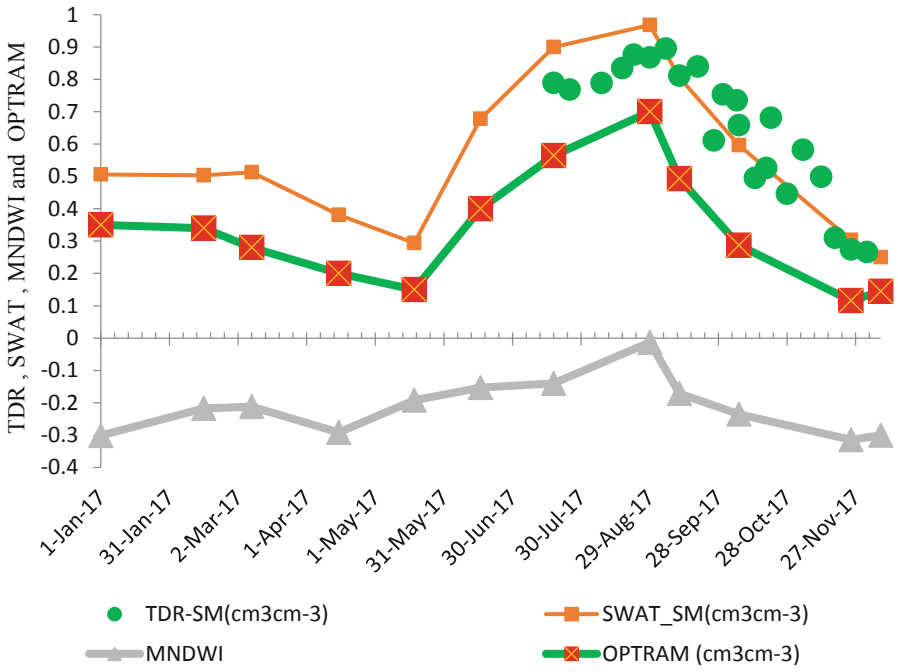

Fig. 9. Time series soil moisture product in TDR, SWAT, MNDWI and OPTRAM

Table 12. Model evaluation

Model	NSE	R^2	PBIAS	RMSE
SWAT	0.51	0.77	−0.24	0.19
OPTRAM	0.61	0.73	0.19	0.025
MNDWI	0.75	−7.98	0.81	132.83

According to the common performance criteria's OPTRAM is relatively the best method to estimate soil moisture in the catchment.

4 Conclusions and Recommendation

4.1 Conclusion

SWAT model sensitivity analysis, it indicated that CN2, ALPHA_BF, GWQMN and ESCO were the most sensitive parameters and has a great impact on stream flow and

soil moisture content. The new OPtical TRApezoid Model (OPTRA M) proposed in this study offers a novel approach to satellite-based remote sensing of soil moisture. OPTRA M has been derived based on the linear relationship between STR and surface soil moisture in bare or vegetated soils. OP-TRAM parameters for a given area can be determined either based on the pixel distribution with-in the STR-NDVI space or with least square regression of the model to field observations. The achievable prediction accuracy of OPTRA M is comparable with the TDR probe. OPTRA M using sentinel 2A level 1C image perform well having NSE (0.61), R^2 (0.73), PBIAS (0.19) and RMSE (0.025). The ESA Sentinel Data Hub at the level 1C processing level (Top-of-Atmosphere radiance) MNDWI spectral index extracted from green (560 nm) and SWIR (2160 nm) bands. NDVI and MNDWI values are well correlated even though the mean vegetation index was less than 0.49, whereas the MNDWI spectral index was less than −0.013. But in all cases, the spectral index has higher reflectance in summer season and low in the dry season. The overall results revealed that SWAT, OPTRA M and MNDWI were capable of simulating soil moisture in daily base. The spatial variation of soil moisture was higher in the TDR probe, and the temporal variation was higher for the MNDWI model. The satellite soil moisture underestimates the In-situ and SWAT modeled moistures. The result indicates that validation of three models with in situ data generally leads to acceptable accuracy having 0.0027 $cm^3\ cm^{-3}$ and 0.0022 $cm^3\ cm^{-3}$ and .034 $cm^3\ cm^{-3}$ standard errors respectively.

4.2 Recommendation

Soil moisture estimation using SWAT semi distributed hydrological model will give accurate result with stream flow data with successful calibration and validation. The depth of soil moisture measurement can be reduced to 5 cm and better approximation can be found with the satellite. Formulating universal dry and wet edge parameter is essential for the better optical trapezoidal model using long term NDVI and STR indexes. Sentinel 2 soil moisture product using visual trapezoidal model should be used to calibrate and validate hydrological models for soil moisture estimation. Even though MNDWI is designed to extract the water body, the index also used to monitor soil moisture status.

Acknowledgements. The authors gratefully acknowledge Bahir Dar University and university of Connecticut for the research fund through its PIRE project. The authors also acknowledge European satellite agency (ESA) for enabling free sentinel images, National Meteorology Agency (NMA) of Ethiopia, and university of Gondar. The three anonymous reviewers and editors are gratefully acknowledged for their valuable comments on our manuscript.

References

1. Falkenmark, M., Rockström, J.: The new blue and green water paradigm: breaking new ground for water resources planning and management. J. Water Resour. Plann. Manage. **132**(3), 129–132 (2006)
2. Chen, H., Shao, M., Li, Y.: The characteristics of soil water cycle and water balance on steep grassland under natural and simulated rainfall conditions in the Loess Plateau of China. J. Hydrol. **360**(1–4), 242–251 (2008)

3. Brocca, L., et al.: Soil moisture estimation through ASCAT and AMSR-E sensors: an intercomparison and validation study across Europe. Remote Sens. Environ. **115**(12), 3390–3408 (2011)
4. Zhang, Q., Shi, Y., Zhu, R.: The study on landslide monitoring with TDR technology. Chin. J. Geol. Hazard Control **6**(2), 67–69 (2001)
5. Narasimhan, B., Srinivasan, R.: Development and evaluation of soil moisture deficit index (SMDI) and evapotranspiration deficit index (ETDI) for agricultural drought monitoring. Agric. For. Meteorol. **133**(1–4), 69–88 (2005)
6. Abate, M., et al.: Morphological changes of Gumara River channel over 50 years, upper Blue Nile basin, Ethiopia. J. Hydrol. **525**, 152–164 (2015)
7. Koster, R.D., et al.: On the nature of soil moisture in land surface models. J. Clim. **22**(16), 4322–4335 (2009)
8. Alexandridis, T.K., et al.: Spatial and temporal distribution of soil moisture at the catchment scale using remotely-sensed energy fluxes. Water **8**(1), 32 (2016)
9. Baghdadi, N., et al.: Analysis of TerraSAR-X data and their sensitivity to soil surface parameters over bare agricultural fields. Remote Sens. Environ. **112**(12), 4370–4379 (2008)
10. Entekhabi, D., et al.: The soil moisture active passive (SMAP) mission. Proc. IEEE **98**(5), 704–716 (2010)
11. Arnold, J.G., et al.: Large area hydrologic modeling and assessment part I: model development 1. JAWRA J. Am. Water Resour. Assoc. **34**(1), 73–89 (1998)
12. Yacoub, C., Foguet, A.P.: Slope effects on SWAT modeling in a mountainous basin. J. Hydrol. Eng. **18**(12), 1663–1673 (2012)
13. Sadeghi, M., et al.: The optical trapezoid model: a novel approach to remote sensing of soil moisture applied to Sentinel-2 and Landsat-8 observations. Remote Sens. Environ. **198**, 52–68 (2017)
14. Kubelka, P., Munk, F.: An article on optics of paint layers. Z. Tech. Phys. **12**(593–601) (1931)
15. Korhonen, L., Packalen, P., Rautiainen, M.: Comparison of Sentinel-2 and Landsat 8 in the estimation of boreal forest canopy cover and leaf area index. Remote Sens. Environ. **195**, 259–274 (2017)
16. Babiker, I.S., et al.: A GIS-based DRASTIC model for assessing aquifer vulnerability in Kakamigahara Heights, Gifu Prefecture, central Japan. Sci. Total Environ. **345**(1–3), 127–140 (2005)
17. Kindie, A.T., Enku, T., Moges, M.A., Geremew, B.S., Atinkut, H.B.: Spatial analysis of groundwater potential using GIS based multi criteria decision analysis method in Lake Tana basin, Ethiopia. In: Zimale, F.A., Enku Nigussie, T., Fanta, S.W. (eds.) ICAST 2018. LNICST, vol. 274, pp. 439–456. Springer, Cham (2019). https://doi.org/10.1007/978-3-030-15357-1_37
18. Lodwick, W.A., Monson, W., Svoboda, L.: Attribute error and sensitivity analysis of map operations in geographical informations systems: suitability analysis. Int. J. Geogr. Inf. Syst. **4**(4), 413–428 (1990)
19. McFeeters, S.K.: The use of the normalized difference water index (NDWI) in the delineation of open water features. Int. J. Remote Sens. **17**(7), 1425–1432 (1996)
20. Setegn, S.G., Srinivasan, R., Dargahi, B.: Hydrological modelling in the Lake Tana Basin, Ethiopia using SWAT model. Open Hydrol. J. **2**(1), 49–62 (2008)
21. Abbaspour, K.C., et al.: Modelling hydrology and water quality in the pre-alpine/alpine Thur watershed using SWAT. J. Hydrol. **333**(2), 413–430 (2007)
22. Moges, M.A., et al.: Suitability of watershed models to predict distributed hydrologic response in the Awramba watershed in lake Tana basin. Land Degrad. Dev. **28**(4), 1386–1397 (2017)
23. Asres, M.T., Awulachew, S.B.: SWAT based runoff and sediment yield modelling: a case study of the Gumera watershed in the Blue Nile basin. Ecohydrol. Hydrobiol. **10**(2–4), 191–199 (2010)

24. Han, E., Merwade, V., Heathman, G.C.: Implementation of surface soil moisture data assimilation with watershed scale distributed hydrological model. J. Hydrol. **416**, 98–117 (2012)
25. Babaeian, E., et al.: A novel optical model for remote sensing of near-surface soil moisture. In: AGU Fall Meeting Abstracts (2016)
26. Gitelson, A.A., et al.: Novel algorithms for remote estimation of vegetation fraction. Remote Sens. Environ. **80**(1), 76–87 (2002)
27. Szabó, S., Gacsi, Z., Balázs, B.: Specific features of NDVI, NDWI and MNDWI as reflected in land cover categories. Acta Geogr. Debrecina Landsc. Environ. **10**(3–4), 194–202 (2016)